# Passive Damping Augmentation For Vibration Suppression In Flexible Latticed Beam-like Space Structures

**Article** *in* Journal of Sound and Vibration · August 1994

DOI: 10.1006/jsvi.1994.1332

CITATIONS
11

READS
53

**2 authors:**

Kelly Cohen
University of Cincinnati
**214** PUBLICATIONS **1,035** CITATIONS
SEE PROFILE

T. Weller
Technion - Israel Institute of Tec…
**93** PUBLICATIONS **808** CITATIONS
SEE PROFILE

*Journal of Sound and Vibration* (1994) **175**(3), 333–346

# PASSIVE DAMPING AUGMENTATION FOR VIBRATION SUPPRESSION IN FLEXIBLE LATTICED BEAM-LIKE SPACE STRUCTURES

K. COHEN AND T. WELLER

*Faculty of Aerospace Engineering, Technion—Israel Institute of Technology, Haifa* 32000, *Israel*

(*Received* 22 *May* 1992, *and in final form* 25 *March* 1993)

For a Timoshenko beam model the equations of motion, representing the anisotropic continuum model of a two-dimensional, latticed, large space structure, are extended to include coupling between the extensional, shear and bending modes. This analytical model, applied to a 20-bay, orthogonal, tetrahedral, cantilevered truss structure, is used to determine the transient response when subjected to a unit impulse. It is demonstrated that for beam-like structures having a fixed bending stiffness and beam mass an increase in diagonal stiffness, on account of the stiffness of the vertical girder, leads to a rise in the transverse shear rigidity. This results in higher natural frequencies and a reduction in peak displacement. In addition, in an asymmetrical truss configuration, coupling between the extensional and shear modes raises the maximum peak displacement compared to that obtained for a symmetric truss. The model is modified to investigate the introduction of passive damping in the form of several dynamic vibration absorbers. For a fixed absorber mass budget, a simple yet efficient absorber parameter optimization procedure, based on the classical steady state criteria of a 2-DOF system, is developed to design several absorbers each tuned to a different modal frequency. It is found that inclusion of transverse shear rigidity, as a design parameter in damping augmentation studies, reduces settling time for predetermined maximum peak displacements.

## 1. INTRODUCTION

Future ventures into outer space include concepts such as large space stations, high resolution radars and communication antennas, astronomical observatories, solar power stations, and space defense platforms. Qualifying as large space structures (L.S.S.), these facilities are generally comprised of repetitive latticed trusses, span large areas with a few intermediate supports, are light in weight and extremely flexible, and consequently are characterized by a large number of high density low frequency structural modes. Besides, L.S.S. require design for very low gravitational environment.

Dynamic verification testing of L.S.S. is very complicated, since it is impossible to include all of the L.S.S. qualities in the test, particularly when performing it in a $1\,g$ environment. Hence, to date, almost all of the experiments conducted have involved structures that are called test beds (terrestrial laboratory structures) possessing *some* desirable qualities of L.S.S. Probably no terrestrial structure will ever have *all* the characteristics of L.S.S., which include high flexibility, low inertia, light inherent damping, as many undamped rigid body modes as possible, low natural frequencies, high modal density, some joint non-linearity, space-qualified sensors, actuators and computers, on-board power, and a laser pointing system. Therefore, sound analytical modeling of the



0022–460X/94/330333 + 14 $8.00/0

structural dynamics problem is of crucial importance since it is complementary to the above experiments.

L.S.S. need to meet target tracking, slewing, stringent line-of-sight and jitter control, pointing accuracies, and microgravity acceleration requirements. However, when disturbed, the structure is likely to remain excited for some time because of its high structural modal density at low frequencies and possibly small damping. It is vital, therefore, to introduce means for passive energy dissipation, active control, or their combination to restrain the response of a given structure within an "in-mission displacement–time allowables envelope" by using vibration control methods.

In passive control, vibrational energy may be dissipated by employing passive methods, with viscoelastic materials that cause material damping used at joints, or as additive layers. Tuned mass dampers and impact/friction forces at structural joints are other efficient sources of passive energy dissipation. These methods have proved to be relatively cheap, simple, reliable and inherently stable. Active vibration suppression techniques for damping augmentation are comprised of sensors and actuators which counteract the effects of the applied loads and disturbances, and require external power sources. Experimental studies with complex structures, however, have shown that the realities of plant model inaccuracies and *real* sensor and actuator dynamics frequently combine to produce disappointing results [1].

Neither passive control alone nor active control alone provide complete vibration control. Experience has proved that the application of passive damping technology to a finite bandwidth actively controlled structure provides essential stabilization and enhances performance by reducing the burden on the active systems. Recent studies conducted on the passive and active control of space structures (PACOSS) have further emphasized the importance of introducing passive means. The best L.S.S. control strategy was found to be a combination of active and passive methods. Designing a predictable amount of passive damping into a structure was proved to be feasible and it was shown that introduction of passive damping can reduce the expenditure of active control energy by 80% to more than 99·9% [2].

L.S.S. such as those intended for the space stations are asymmetric and therefore the effects of bending, shear, torsion and longitudinal motion are coupled. At present, there is little information on the advantages, trade-offs and limitations of these couplings in the vibration suppression of large space structures.

According to the detailed literature survey given in reference [1], the problem of undesirable vibrational energy in large, flexible, beam-like repetitive lattices of non-symmetric geometry space structures is minimized by augmenting dissipation, using passive means in the form of dynamic vibration absorbers. Whereas recent efforts have been con centrated on using tuned mass dampers for vibration suppression of L.S.S. with models possessing a number of discrete (non-continuous) degrees of freedom [3], or in systems having symmetric configurations [4], the present study is of a continuous, 20-bay, latticed beam-like structure for which the effects of asymmetry and resident transverse shear on the structural dynamic problem are first examined. Later, a unique procedure for obtaining optimal tuning and damping parameters of several absorbers is applied to a cantilevered truss in order to minimize the settling time of the transient, transverse displacement response.

## 2. EQUATIONS OF MOTION

In this section the equations of motion of a Timoshenko beam model, which includes coupling between the extensional, bending and shear modes, is modified to include the attachment of dynamic vibration absorbers.

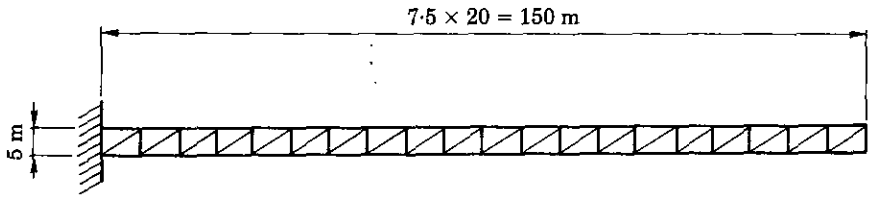


Figure 1. A 2-D version of the orthogonal tetrahedral lattice.

A two-dimensional version of the orthogonal tetrahedral configuration (non-symmetric) is considered (see Figure 1). These trusses are primary candidates for a space station [5]. For the lattice shown in Figure 1, the smallest possible repeating cell, which may be isolated from the grid, extends over one bay of the original structure (see Figure 2). The equivalent continuum beam properties, stiffness coefficients and density parameters, for the plane strain case, have been computed by performing the static tests described in reference [6]. This results in the constitutive relations:

$$\begin{bmatrix} N \\ M \\ Q \end{bmatrix} = \begin{bmatrix} C_{11} & 0 & C_{13} \\ 0 & C_{22} & 0 \\ C_{13} & 0 & C_{33} \end{bmatrix} \begin{bmatrix} \epsilon_x^0 \\ k_z^0 \\ 2\epsilon_{xz}^0 \end{bmatrix}, \tag{1}$$

where $N$, $M$ and $Q$ are the extensional force, the bending moment and the transverse shear force respectively (see Figure 3) and $[C_{ij}]$ is the stiffness matrix of the continuum beam element (see Figure 3), $\epsilon_x^0$ is the extensional strain, $k_z^0$ is the curvature change of the beam, $\epsilon_{xz}^0$ is the transverse shear strain, and $C_{13}$ is the coupling between the extensional and transverse shear stiffness. (Calculations of $C_{ij}$ indicate that $[C_{ij}]$ is symmetric. Also, note that for trusses with identical upper and lower longerons, it has been shown [6] that $C_{12} = C_{23} = 0$.) Also, the matrix of material densities is given by

$$[m] = \begin{bmatrix} m_{xx} & 0 & 0 \\ 0 & m_{\theta\theta} & 0 \\ 0 & 0 & m_{zz} \end{bmatrix}. \tag{2}$$

During this study, the lattice geometry, structural mass $[m_{ij}]$ and transverse bending rigidity are fixed: i.e., the Euler–Bernoulli model remains identical! The stiffness properties $C_{11}$, $C_{13}$ and $C_{33}$ are varied by using the non-dimensional geometric coefficient

$$\beta = (2^* Ad/Ag), \tag{3}$$

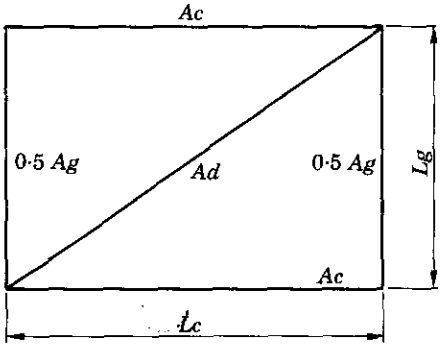


Figure 2. The repeating cell of the asymmetric lattice.

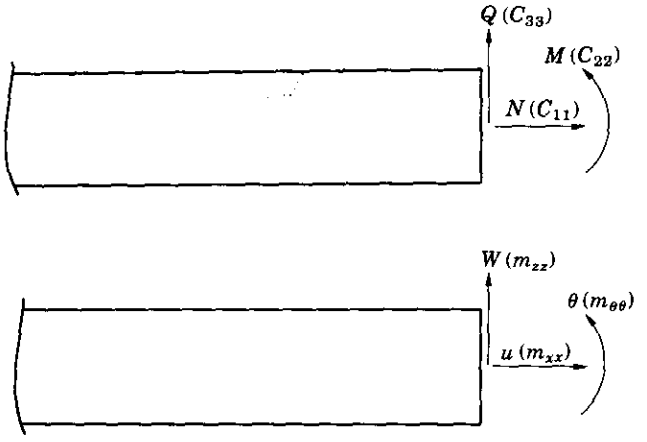


Figure 3. The simplified beam element and sign convention.

where $Ad$ and $Ag$ are the cross-sectional areas of the diagonal and vertical members of the truss depicted in Figure 2.

For the static tests [6] small displacements are assumed to obtain the values of the matrix $[C_{ij}^*]$ (where $[C_{ij}]^{-1} = [C_{ij}^*]$). Since the theory of continuum modeling presented here is based on linear elasticity, it is imperative to restrict $\beta$, during the parametric study, only to those values for which the assumption of linearity is justified. For this reason, a method was devised whereby the equivalent beam properties, $C_{13}^*$ and $C_{33}^*$, corresponding to the plain strain case were computed, by using the COSMOS/M finite element program [7], for both non-linear and linear responses induced by a static shear force. Thus, the application of the continuum model developed by Sun [6] is restricted only to the values of $\beta$ which comply with the requirement of linear behavior. Following the study conducted by Cohen and Weller [1], $\beta$ was varied within the region $1{\cdot}33 \leqslant \beta \leqslant 3{\cdot}00$.

The effect of the coupling factor, $C_{13}$, is evaluated for the repeating cell depicted in Figure 4, for which:

$$Ad1 + Ad2 = Ad, \tag{4}$$

where $Ad1$ and $Ad2$ are the cross-sectional areas of the diagonal members of the truss (see Figure 4). For simplicity, the following, non-dimensional geometric coefficient is defined:

$$\beta^* = (Ad1/Ad2). \tag{5}$$

By varying values of $Ad1$ and $Ad2$ in equation (4) (i.e., $\beta^*$), the structural dynamics problem of the symmetrical L.S.S. ($\beta^* = 1$) can be compared to that of the asymmetric configuration (where in the extreme case $\beta^* = 0$).

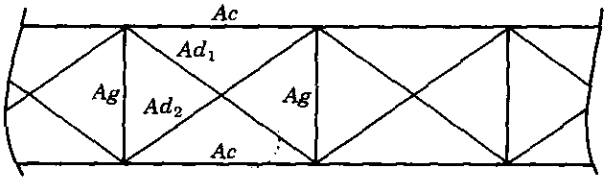


Figure 4. The repeating cell of the truss for examining the effects of asymmetry.

For a Timoshenko beam, the equations of motion, representing an anisotropic continuum model of a two-dimensional latticed structure, form a set of three coupled partial differential equations with the displacement variables $u(x, t)$, $(w(x, t)$ and $\Theta(x, t)$:

$$C_{22}(\partial^2\Theta/\partial x^2) + C_{13}(\partial u/\partial x) + C_{33}(\partial w/\partial x) - m_{\theta\theta}(\partial^2\Theta/\partial t^2) = C_{33}\Theta, \tag{6}$$

$$C_{11}(\partial^2 u/\partial x^2) + C_{13}(\partial^2 w/\partial x^2) - C_{13}(\partial\Theta/\partial x) - m_{xx}(\partial^2 u/\partial t^2) = 0, \tag{7}$$

$$C_{13}(\partial^2 u/\partial x^2) + C_{33}(\partial^2 w/\partial x^2) - C_{33}(\partial\Theta/\partial x) - m_{zz}(\partial^2 w/\partial t^2) = 0. \tag{8}$$

The natural frequencies and mode shapes of the vibrating anisotropic beam have been obtained numerically, for various values of $\beta$ and $\beta^*$, with use of a spreadsheet, by solving the eigenvalue problem, which is a $6 \times 6$ determinantal frequency equation. The procedure was validated in reference [1], by comparing values obtained by applying a spreadsheet with those computed by using the COSMOS/M finite element program [7], as well as with those displayed in reference [6].

Transient disturbances, modeled as initial conditions and corresponding to a unit impulse, may simulate shuttle docking or crew motion [3]. A linear dynamic analysis of the truss, based on the normal mode method, evaluates the response at time $t$ by integrating the uncoupled equations of motion from time zero to time $t$. The size of the time step increment, which is a key factor in the accuracy of the results, and the total number of modes included in the analysis obviously affect the accuracy. However, this improvement is at the cost of complexity and solution time. Therefore, the value of the time step and the number of modes required need to be selected in compliance with the adequacy of the solution.

Finally, when $n$ dynamic vibration absorbers are attached to the beam-like structure at a distance $a_i$ $(i = 1, \ldots, n)$ from the origin (see Figure 5), equation (8) becomes:

$$C_{13}(\partial^2 u/\partial x^2) + C_{33}(\partial^2 w/\partial x^2) - C_{33}(\partial\Theta/\partial x) - \sum_{i=1}^{n}\left[c_i\left\{\frac{dq_i}{dr} - \frac{\partial w(a_i, t)}{\partial t}\right\}\right.$$

$$\left. + k_i\{q_i - w(a_i, t)\}\right]\delta(x - a_i) - m_{zz}\frac{\partial^2 w}{\partial t^2} = 0, \tag{9}$$

where $\delta(x - a_i)$ is the Dirac delta function for $i = 1, \ldots, n$, and $k_i$ and $c_i$ are the stiffness and damping constants of the $i$th absorber, respectively. The displacement of the $i$th

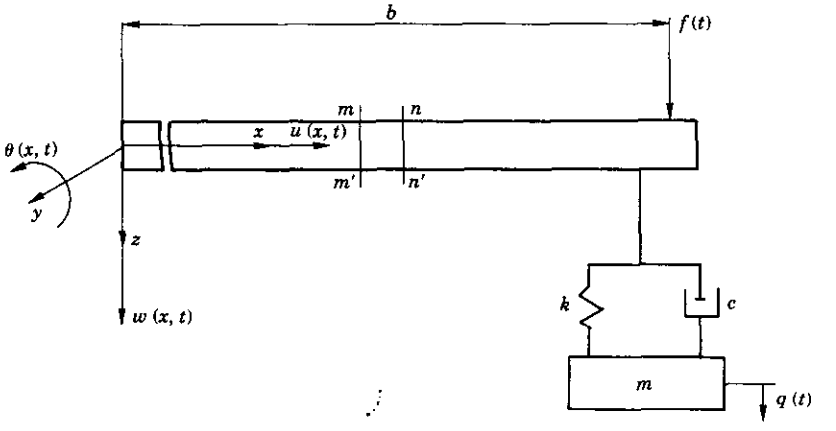


Figure 5. The cantilever beam with the dynamic absorber attached.

absorber in the $z$ direction is denoted by the variable $q_i$. Then, the equation of motion of any absorber is

$$m_i(\mathrm{d}^2q_i(t)/\mathrm{d}t^2) + c_i[(\mathrm{d}q_i(t)/\mathrm{d}t) - (\partial w(a_i, t)/\partial t)] + k_i[q_i(t) - w(a_i, t)] = 0. \tag{10}$$

The total mass of the absorbers is kept at 10% of the structural mass of the beam. By the examination of criteria for optimization of the transient response in reference [3], for a 2-DOF system, the optimal tuning ratio was found to be identical to that of the steady state (S.S.) minimized solution [8]. The ratio of the frequency of the $i$th tuned mass damper to the $i$th natural frequency, $To_i$, is obtained by equating the first two peaks of the S.S. response:

$$To_i = \frac{1}{[1 + \mu_i w_i^2(l)]}. \tag{11}$$

$To_i$ is referred to as the "tuning ratio" and $\mu_i$ is the ratio of the absorber mass to the structural mass of the latticed beam-like structure. The value of $w_i(l)$ is obtained from the characteristic function representing the respective mode of an Euler–Bernoulli beam of appropriate boundary conditions. In this case, when tuning the absorbers to the first two modes, $w_i(l)$ is obtained for the $i$th mode of the cantilever beam. (In Table 4 of section 3 it is shown that the first two modes are the major contributors (98·5%) to the transient response.) The implementation of equation (11) for tuning of an absorber attached to a truss was found to be simple, time-saving and efficient [1].

Damping is introduced into the system in the form of concentrated viscous dampers, placed at points where maximum modal displacement occur for the truss and the absorber masses. These dampers apply a force which is proportional to the relative nodal velocities, $\dot{w}_i^{rel}$, between the point of absorber attachment to the beam and the mass of the undamped absorber. The damper force, $F_d^i$ is therefore

$$F_d^i = c_i \dot{w}_i^{rel}, \tag{12}$$

where $c_i$ is a given constant of proportionality called the damper constant and $\dot{w}_i^{rel}$ is obtained from the response of the system. The dampers are modeled, by using the COSMOS/M program, in such a manner that their inclusion does not affect the frequency solution for the lattice with undamped absorbers. The effect of the dampers (irrespective of the fact that damping may be non-proportional) is considered in the modal analysis by applying assumed external forces $F_{ex}^i$ on the combined "beam"-undamped absorbers configuration. The product of the relative nodal velocities, with the defined damping coefficient of the absorber, $c_i$, is equated to the above assumed external force. This numerical process is continued by performing iterations at each time step of the solution until convergence is reached when the assumed force yields nearly the same damper force obtained from the response of the system (i.e., $F_{ex}^i = F_d^i$).

The method of obtaining the optimal tuning and damping parameters of several absorbers, attached to a vibrating truss, is shown in Figure 6. The criterion for selecting the above parameters is the requirement that the minimal settling time be reached for a predetermined value of the maximum absolute peak displacement.

## 3. RESULTS

This effort is aimed at achieving two objectives. First, before introduction of passive means of vibrational control, the effects of shear and asymmetry in minimizing the absolute peak transverse deflection response are examined. Later, with the addition of dynamic vibration absorbers, application of a unique and efficient and accurate iterative procedure

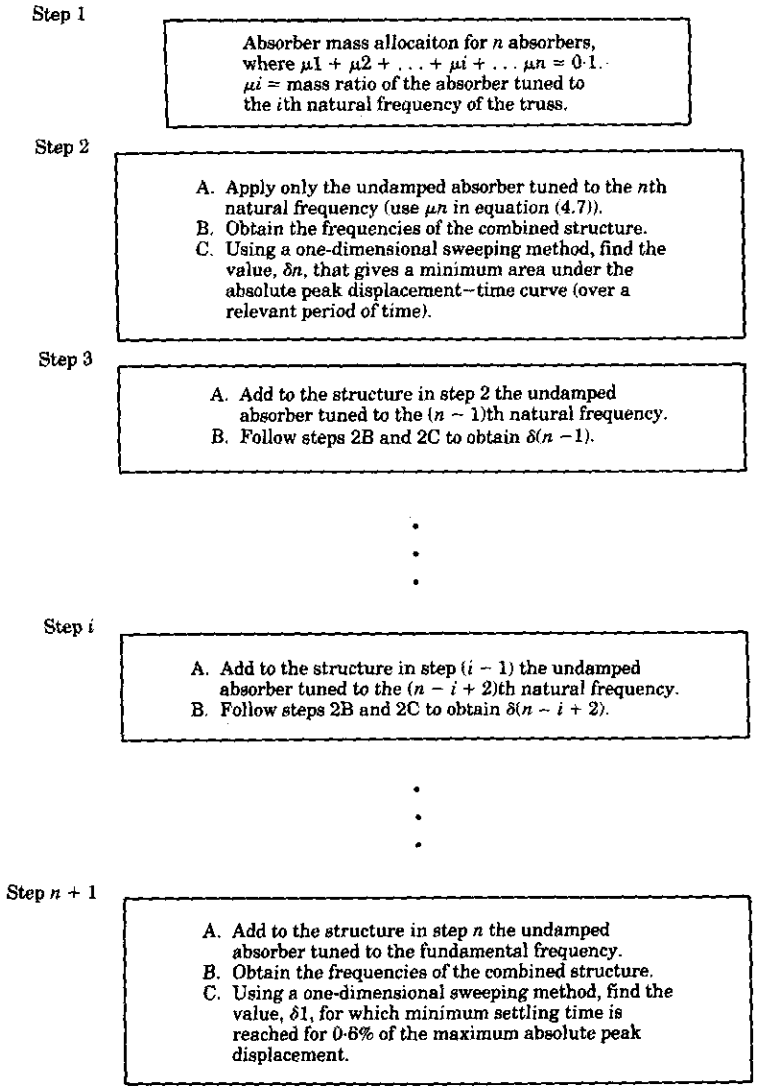


Figure 6. The flowchart for obtaining the optimal tuning and damping parameters for several absorbers attached to the truss.

for computing the design parameters of the absorber, which are required to reach 0·6% of the maximum undamped absolute peak displacement in minimum time, is demonstrated.

The repeating cell of the lattice, which is a 2-D version of the orthogonal tetrahedral lattice (see Figure 2), is defined by the following parameters: $Lc = 7{\cdot}5$ m, $Lg = 5$ m, $Ac = 80 \times 10^{-6}$ m$^2$, $Ad = 40 \times 10^{-6}$ m$^2$, $Ag = 60 \times 10^{-6}$ m$^2$, $\sigma = 2768$ kg/m$^3$ (density of all truss members), and $E = 71{\cdot}7 \times 10^9$ N/m$^2$ (Young's modulus of all truss members).

In order to arrive at the values of the matrix $[C_{ij}^*]$, the assumption of linearity in truss deflection needs to be justified. The equivalent continuum beam properties, $C_{13}^*$ and $C_{33}^*$, corresponding to the plane strain case, were computed with the COSMOS/M program [7] by using the method developed by Sun [6]. In Table 1 the eigenfrequencies are compared with those of reference [6], where a higher order Timoshenko beam finite element analysis was used, which takes into account coupling among the three basic deformations $u$, $w$ and $\Theta$. The first four modes yielded by an equivalent Euler–Bernoulli beam were also included,

TABLE 1

*Natural frequencies of asymmetric truss for* $\beta = 1{\cdot}33$ rad/s

| Mode | FEM [6] | Timoshenko [6] | COSMOS/M [7] | Continuum model spreadsheet | Euler–Bernoulli |
|---|---|---|---|---|---|
| 1 | 1·5626 | 1·576 | 1·5626 | 1·572 | 1·593 |
| 2 | 9·1179 | 9·206 | 9·1179 | 9·173 | 9·982 |
| 3 | 23·222 | 23·460 | 23·2222 | 23·340 | 27·954 |
| 4 | 40·289 | 40·767 | 40·2888 | 40·472 | 54·779 |
| 5 | 43·357 | 43·740 | 43·3573 | 43·541 | — |

and it is apparent that the discrepancy between them and the ones corresponding to the Timoshenko beam justifies the efforts involved in using the Timoshenko beam model. For comparison, the original truss structure was modeled and computed by the COSMOS/M program. It should be noted that mode 5 is a longitudinal mode. Comparisons in Table 1 validate the continuum type model used for the analysis of anisotropic beam-like lattice trusses.

The matrix $[C_{ij}]$, computed for different values of $\beta$, is presented in Table 2. It should be noted that the bending stiffness, $C_{22}$, is constant (and therefore not given in Table 2), while the variations in the axial stiffness, $C_{11}$, are slight when compared to those in $C_{13}$ and $C_{33}$. It is apparent from Table 2 that the values of $C_{13}$ and $C_{33}$ increase with increasing $\beta$ values, resulting in a stiffer structure. Consequently, the resulting natural frequencies, increase with $\beta$ (which, in fact, represents an increase in diagonal stiffness, on account of the stiffness of the vertical girder) for a constant structural mass. As a result of this phenomenon the fundamental frequency for $\beta = 3{\cdot}0$ is 1·5708 rad/s as compared with 1·5626 rad/s for $\beta = 1{\cdot}33$. Thus, an increase in diagonal stiffness, on account of the stiffness of the vertical girder, leads to a rise in the shear coefficients, $C_{13}$, and $C_{33}$.

In an asymmetrical truss, coupling between the extensional and shear modes lowers the value of equivalent shear rigidity as compared to that of a symmetric truss, thus lowering the natural frequencies. It is evident from Figure 7 that coupling between the longitudinal and shear modes is at its highest for the asymmetric truss when $\beta^* = 0$. On the other hand, in the symmetric case all the $C_{ij}$ matrix coefficients, where $i \neq j$, of the 2-D structure are uncoupled. In addition, the shear coefficient, $C_{33}$, is higher for $\beta^* = 1$ than those corresponding to non-symmetric configurations, $\beta^* < 1$.

From reference [1], it was verified that for the linear dynamic analysis of the 20-bay truss structure, depicted in Figure 1, an appropriate selection of the time step used in the integration of the uncoupled equations of motion is 0·1 s (well below 1/10th of the first natural period of the structure—6·41 s), since the response obtained for this time increment

TABLE 2

*The effect of* $\beta$ *on matrix* $[C_{ij}]$

| $\beta$ | $Ag$ ($10^{-6}$ m$^2$) | $Ad$ ($10^{-6}$ m$^2$) | $C_{11}$ ($10^6$ N) | $C_{13}$ ($10^{-6}$ N) | $C_{33}$ ($10^6$ N) |
|---|---|---|---|---|---|
| 1·33 | 60·0 | 40·0 | 12·955 | 0·989 | 0·659 |
| 1·61 | 53·8 | 43·4 | 13·047 | 1·050 | 0·700 |
| 1·78 | 50·8 | 45·1 | 13·090 | 1·078 | 0·718 |
| 2·09 | 45·8 | 47·8 | 13·148 | 1·117 | 0·745 |
| 2·40 | 41·8 | 50·1 | 13·190 | 1·145 | 0·763 |
| 3·00 | 35·6 | 53·4 | 13·228 | 1·171 | 0·780 |

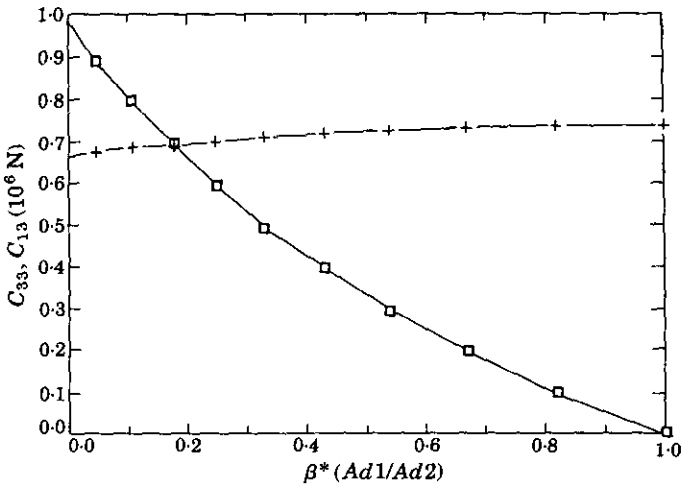


Figure 7. The effects of asymmetry: shear coefficients *vs.* $\beta^*$. □, $C_{13}$; +, $C_{33}$.

is acceptable when compared to that reached with time step increments of either 0·05 s or 0·01 s. In addition, it was also shown that the number of modes required before truncation, 5, is adequate.

Transient responses for the symmetric and asymmetric configuration of $\beta = 1{\cdot}33$ are given in Figure 8, and a comparison is made with the asymmetric truss having $\beta = 3{\cdot}0$. Note that the absolute peak transverse deflections given in Figures 8–12 are curves comprised of *only* the absolute values, of *all* the maximum points (peaks) of the displacement response, $w(l, t)$. The peak displacement response, measured at the free end of the cantilever, for the asymmetric truss, $\beta = 3{\cdot}0$, is found to be the lowest of the three. The decrease in the absolute peak transverse deflection, for $\beta = 3{\cdot}0$, is due to an increase in the value of the fundamental frequency, 1·5708 rad/s, as against 1·5626 rad/s for $\beta = 1{\cdot}33$ (see Tables 1–6). Therefore, an increase in the stiffness of the diagonal member, on account of the stiffness of the vertical girder, leads to a rise in the transverse shear rigidity which corresponds to minimizing the absolute peak transverse deflection. This

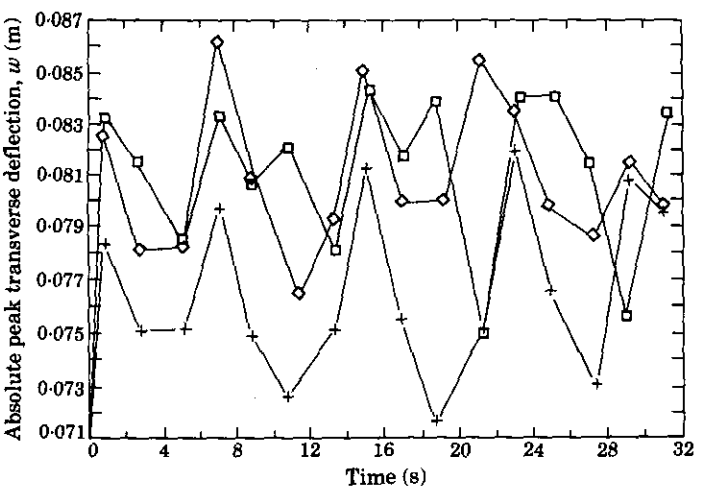


Figure 8. The impulse response envelopes of the undamped truss for various geometric configurations. □, $\beta = 1{\cdot}33$ (asymmetric); +, $\beta = 3{\cdot}00$ (asymmetric); ◇, $\beta = 1{\cdot}33$ (symmetric).

TABLE 3

*Peak impulse longitudinal and transverse responses*

| Symmetric ($\beta^* = 1{\cdot}0$) | | | Non-symmetric ($\beta^* = 0{\cdot}67$) | | |
|---|---|---|---|---|---|
| Time (s) | $w$ (m) | $u$ (m) | Time (s) | $w$ (m) | $u$ (m) |
| 0·85 | 0·0844 | 0·0028 | 0·85 | 0·0844 | 0·0028 |
| 3·13 | −0·0830 | −0·0031 | 3·12 | −0·0830 | −0·0029 |
| 4·86 | 0·0837 | 0·0030 | 4·85 | 0·0835 | 0·0030 |
| 7·33 | −0·0798 | −0·0032 | 7·32 | −0·0808 | −0·0032 |
| 9·05 | 0·0888 | 0·0034 | 9·03 | 0·0892 | 0·0034 |
| 10·77 | −0·0819 | −0·0034 | 10·75 | −0·0818 | −0·0032 |
| 13·04 | 0·0838 | 0·0024 | 13·06 | 0·0852 | 0·0029 |
| 14·95 | −0·0743 | −0·0019 | 14·92 | −0·0783 | −0·0026 |

makes the inclusion of the transverse shear rigidity an important design parameter in transient, damping augmentation studies of large space structures. Calculations show that, for $\beta = 1{\cdot}33$, the area under the displacement–time curve of the symmetric lattice is slightly smaller than that of the asymmetric one.

For $\beta = 1{\cdot}33$, a unit impulse applied on a symmetric truss, $\beta^* = 1{\cdot}0$, as well as a non-symmetric truss, $\beta^* = 0{\cdot}67$, leads to extensional deflections, $u(t)$, of an order of 5% of the transverse deflections, $w(t)$: i.e., $u(t)/w(t) < 0{\cdot}05$. It can be seen from Table 3 that the inclusion of coupling between the transverse shear and the longitudinal extension, reflected by the coefficient $C_{13}$, has an adverse effect on the maximum peak displacement.

### 3.1. ONE ABSORBER ONLY

Classical steady state criteria [8] are used to tune the absorber (having an allocated mass budget of 10%) to the fundamental frequency of the Euler–Bernoulli beam. The normalized impulse response envelopes for various damping ratios for $\beta = 1{\cdot}33$ and $3{\cdot}0$ are given in Figures 9 and 10, respectively. In both cases the damper value which minimizes settling time is reached for a damping ratio $\delta o = 0{\cdot}5$. The settling time for achieving 5% of the maximum peak displacement, for the asymmetric truss (of reference [6]), $\beta = 1{\cdot}33$,

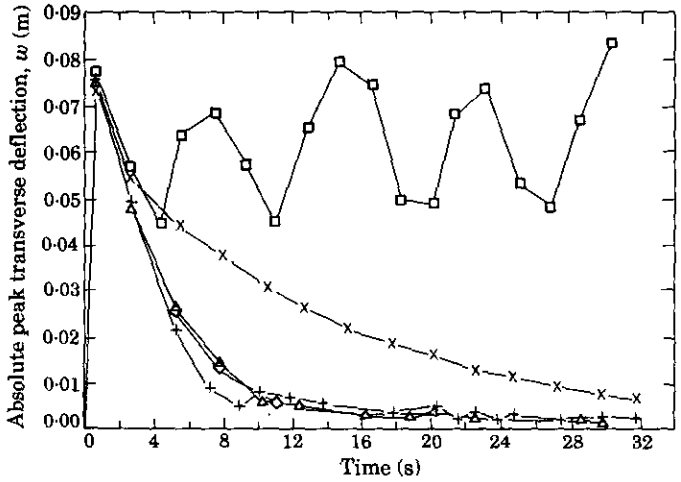


Figure 9. The impulse response envelopes for various damping ratios ($\beta = 1{\cdot}33$). □, $\delta = 0{\cdot}00$; +, $\delta = 0{\cdot}37$; ◇, $\delta = 0{\cdot}47$; △, $\delta = 0{\cdot}50$; ×, $\delta = 1{\cdot}50$.

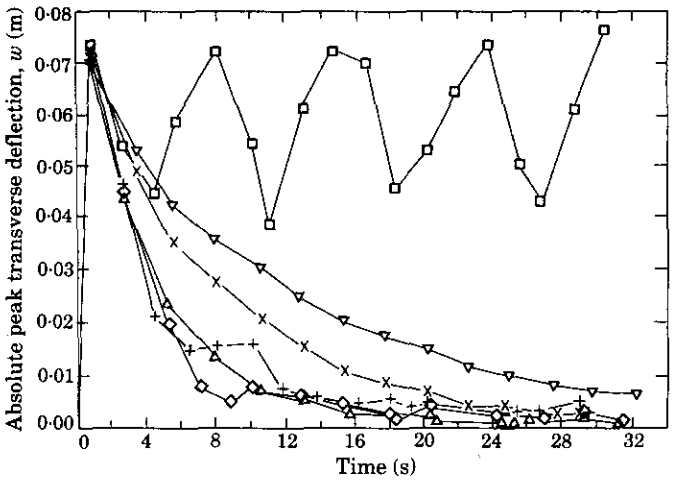


Figure 10. The impulse response envelopes for various damping ratios ($\beta = 3{\cdot}00$). □, $\delta = 0{\cdot}00$; +, $\delta = 0{\cdot}25$; ◇, $\delta = 0{\cdot}37$; △, $\delta = 0{\cdot}50$; ×, $\delta = 0{\cdot}95$; ▽, $\delta = 1{\cdot}50$.

was 21 s, whereas for $\beta = 3{\cdot}00$, the settling time was a mere 13 s. It is worthwhile noting in Figures 9 and 10 that a considerable change in the value of the damping ratio, $\delta$, in the neighborhood of $\delta o$ almost does not affect the response of the system. As the value of $\delta$ is increased, a reduction in absorber performance takes place as a result of a high damper force which restrains relative movement of the absorber mass.

### 3.2. TWO ABSORBERS

The most efficient way to apply absorbers is by tuning them only to the modes that make a significant contribution to the transient response. For $\beta = 3{\cdot}0$, in Table 4 are depicted the effects of the respective modes on the absolute peak displacement response curve. For clarity, these effects are presented in non-dimensional form, $R_k$, where $R_k$ is the ratio of the area under the absolute peak transverse displacement–time curve when using the first $k$ modes to the area obtained when using the first 15 modes. The ratio $R_k$ relates to the transverse deflection $w(l, t)$ only. The reason why $R_k$ does not monotonically approach 1·0 may be due to the coupling between the extensional and transverse deflections (modes 5 and 10 are longitudinal modes). However, it can be seen from Table 4 that the main contributors are found to be the first two modes. Therefore, two absorbers, with a total mass equaling 10% of the mass of the truss, attached at the free end of the cantilevered truss, will be tuned to the first two modes.

TABLE 4

*Contribution of modes to transient response*

| Number of modes | $R_k$ |
|---|---|
| 1 | 0·890 |
| 2 | 0·985 |
| 3 | 0·999 |
| 4 | 1·003 |
| 6 | 1·001 |
| 7 | 0·987 |
| 8 | 0·998 |
| 9 | 0·999 |
| 15 | 1·000 |

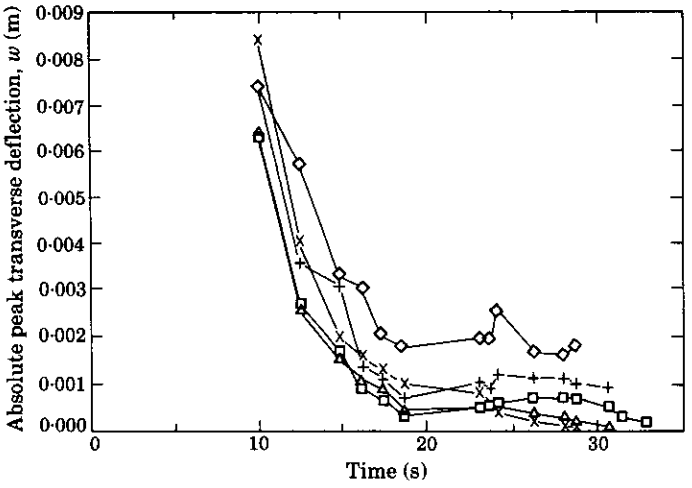


Figure 11. The impulse response envelopes for various absorber mass distributions, $\mu_1$ and $\mu_2$. ◇, $\mu 1 = 0{\cdot}1$; +, $\mu 1 = 0{\cdot}09$; □, $\mu 1 = 0{\cdot}08$; △, $\mu 1 = 0{\cdot}07$; ×, $\mu 1 = 0{\cdot}055$.

By using the method outlined in Figure 6 with values of 0·1, 0·09, 0·08, 0·07 and 0·055 for the mass ratios of the absorber tuned to the fundamental frequency, $\mu 1$, the minimum settling time to reach 0·6% of the maximum undamped absolute peak displacement is reached. Previously, with but one absorber tuned to the fundamental frequency, the requirement of reaching 0·6% of the maximum undamped absolute peak displacement cannot be reached due to the significant contribution of the second mode. From Figure 11, it can be seen that the above minimal settling time, 19 s, is obtained for $\mu 1 = 0{\cdot}07$ and $\mu 2 = 0{\cdot}03$. The curves in Figure 11, being magnified, commence after the first 10 s and they (the curves) also justify the additional absorber tuned to the second frequency. As the value of $\mu 2$ exceeds approximately 0·03, the efficiency of the dual absorber system falls gradually.

As an example, Sesak *et al.* [3] applied two absorbers to suppress the vibration of the pitch rotation (payload pointing response example). The uncoupled dynamic optimization (U.D.O.) method, which yielded the best results, computes the spring and damper constants for each absorber; the tuning laws of a 2-DOF system are used, and no spatial coupling is assumed (i.e., coupling such that the location of an absorber at a maximum of one mode also affects the other mode).

The U.D.O. was applied to a 20-bay truss ($\beta = 3{\cdot}0$, $\mu 1 = 0{\cdot}07$ and $\mu 2 = 0{\cdot}03$) and the response thus obtained is compared with that reached by using the solution presented in Figure 6, the coupled dynamic optimization (C.D.O.) method in Table 5, which highlights the differences and similarities of these two methods.

TABLE 5
*Absorber parameters*

| Parameters | U.D.O. | C.D.O. |
|---|---|---|
| $T_1$ | 0·7813 | 0·7813 |
| $T_2$ | 0·8929 | 0·8929 |
| $K_1$ (N/m) | 10·797 | 9·721 |
| $K_2$ (N/m) | 211·66 | 211·66 |
| $\delta_1$ | 0·50 | 0·38 |
| $\delta_2$ | 0·75 | 0·75 |

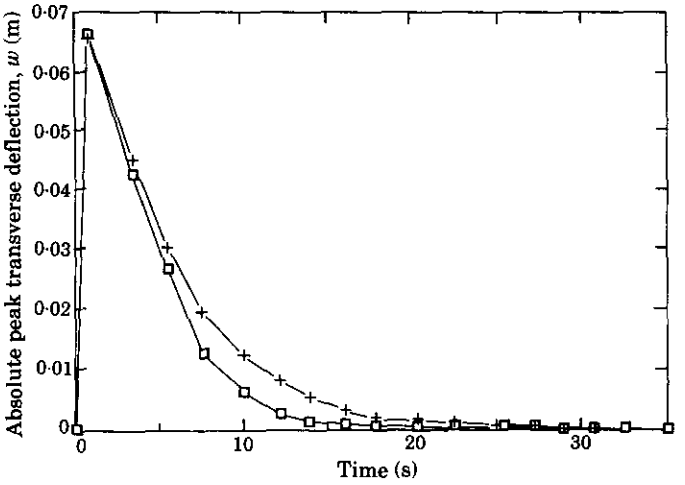


Figure 12. The impulse response envelopes for various absorber parameter optimization methods ($\mu_1 = 0{\cdot}07$, $\mu_2 = 0{\cdot}03$). □, C.D.O. method of Figure 6; +, uncoupled method (U.D.O.).

From Figure 12, it can be seen that the method provided in Figure 6 offers a quicker settling time, 19 s, compared to that obtained by using the U.D.O. method, 30 s. The cause of this difference lies in the calculation of the stiffness of absorber 1, tuned to the fundamental frequency, $k1$. Whereas $k1$ is given by

$$k1 = T_1^2 m_1 \Omega_1^2, \tag{13}$$

the tuning ratios are basically a function of the absorber mass ratio alone. When using Figure 6, the value of $\Omega_1$, used in equation (13), is the fundamental frequency of the combined system consisting of the truss and absorber 2, tuned to the second natural frequency of the truss. From Table 6, it is evident that the introduction of absorber 2 alone, to the truss, affects the value of the first natural frequency significantly whereas the addition of absorber 1 alone has hardly any effect on the values of the higher frequencies. Therefore, tuning of absorber 1 to 1·4826 rad/s gives better results due to the appreciable amount of spatial coupling, caused by the locations of the absorbers at the maxima of the first two modes (free end of the absorber).

TABLE 6

*Natural frequencies for $\beta = 3{\cdot}0$ (rad/s) obtained during the comparison of absorber optimization methods*

| Frequency number of truss | Truss only | Absorber 1 only, $\mu_1 = 0{\cdot}07$ | Absorber 2 only, $\mu_2 = 0{\cdot}03$ | U.D.O. method | C.D.O. method |
|---|---|---|---|---|---|
| Absorber 1 | — | 1·0651 | — | 1·0539 | 1·0202 |
| 1 | 1·5708 | 1·7952 | 1·4826 | 1·7133 | 1·6799 |
| Absorber 2 | — | — | 7·6798 | 7·6825 | 7·6823 |
| 2 | 9·2466 | 9·2672 | 10·4226 | 10·4397 | 10·4380 |
| 3 | 23·7929 | 23·7999 | 23·9546 | 23·9620 | 23·9613 |
| 4 | 41·3662 | 41·3687 | 41·4161 | 41·4185 | 41·4183 |
| 5 | 43·8344 | 43·8356 | 43·8594 | 43·8606 | 43·8606 |

## 4. CONCLUSIONS AND RECOMMENDATIONS

An analytical Timoshenko beam-like model of a 2-D truss, modified to include attached dynamic vibration absorbers, was solved to determine the transient response of a beam-like latticed structure to a unit impulse excitation. The shearing coefficients of the continuum model, $C_{13}$ and $C_{33}$, were found to be useful design parameters which affect the damping augmentation of the L.S.S. The model was modified to investigate the addition of passive damping in the form of dynamic vibration absorbers. For a given mass distribution, the C.D.O. method presented in Figure 6 utilizes the effects of spatial coupling to provide a simple, yet efficient means of determining the stiffness and damping constraints of the absorbers.

The analytical model presented could be further developed to analyze 3-D beam-like and plate-like latticed structures, which include coupling between the bending, transverse shear, twisting and extensional modes. Design procedures concerning the geometric configurations of flexible large space structures, reflected by the parameter $\beta$, could be investigated in a non-linear analysis to provide internal damping mechanisms that would lower the burden on specialized means of damping augmentation. The passive damping mechanisms, discussed in this work, may be introduced into a finite bandwidth, actively controlled structure by using a multi-disciplinary approach.

## ACKNOWLEDGMENT

The work reported in this paper was part of an M.Sc. Thesis submitted by the first author to the Technion—Israel Institute of Technology, in partial fulfillment of the requirements for the M.Sc. degree.

## REFERENCES

1. K. COHEN and T. WELLER 1990 *TAE Report No.* 655 *of the Faculty of Aerospace Engineering, Technion—Israel Institute of Technology*. Passive damping augmentation of flexible beam-like lattice trusses for large space structures.
2. P. J. TORVIK 1990 *Aerospace America* **28**, 44. Structural dynamics.
3. J. R. SESAK, M. J. GRONET and G. M. MARINOS 1987 *NASA* CR 4067, NAS1-17660. Passive stabilization of large space systems.
4. J. N. JUANG 1984 *Journal of Guidance* **7**, 733–739. Optimal design of a passive vibration absorber for a truss beam.
5. A. K. NOOR and M. M. MIKULAS 1988 in *Large Space Structures: Dynamics and Control*, 1–34. Berlin: Springer-Verlag. Continuum modeling of large lattice structures: status and projections.
6. B. NECIB and C. T. SUN 1989 *Journal of Sound and Vibration* **130**, 149–159. Analysis of truss beams using a high order Timoshenko beam finite element.
7. M. LASHKARI 1987 *COSMOS/M User Guide: Stress, Vibration, Buckling, Dynamics, and Heat Transfer Analysis*. Release version 1.5. Structural Research and Analysis Corporation.
8. R. G. JACQUOT 1978 *Journal of Sound and Vibration* **60**, 535–542. Optimal dynamic absorbers for general beam systems.